IJBBE International Journal of Biophotonics & Biomedical Engineering Vol. 4, No. 2, Fall - Winter, 2024

Research Article

Investigating the effect of soluble and insoluble medicinal substances on cell wall orientation

N. Ebrahimpour [a], M. Sadegh Zakerhamidi [b], A. Ranjkesh[c], R. Kian[a,b]

a Department of Chemical Industry, National University of Skills (NUS), Tehran, Iran
b Faculty of Physics, University of Tabriz, Iran
cCondensed Matter Department, J.Stefan Institute, Jmova 39, Ljubljana, Slovenia

***Corresponding Author Email: neda.ebrahimpour@gmail.com**

DOI: 10.71498/ijbbe.2024.1190467

ABSTRACT

Received: Nov. 14, 2024, Revised: Jan. 3, 2025, Accepted: Jan. 26, 2025, Available Online: Feb. 18, 2025

Considering that the cell wall is the first defense and control barrier of medicinal substances into the cell, any dielectric behavior of this divider can lead to harm to the cell or the absorption of substances from the environment; hence, examining the dielectric and physicochemical behavior of the anisotropic cell wall is imperative. The present study employs 1102 (a mixture of liquid crystals) as an anisotropic environment, similar to the cell wall. In insoluble nanoparticles, Lithium disilicate ($Li_2Si_2O_5$) is employed as a non-reactive material, while materials containing active agents are used as soluble materials like Retinol ($C_{20}H_{30}O$). At various dopant concentrations, the dielectric characteristics and optical anisotropies of the liquid crystal and dopant mixture were observed, and the resulting data was analyzed and studied results indicate that the shape of the insoluble dopant influences the molecular order of the liquid crystal bulk, while for soluble substances, the percentage of dopant is more significant than the shape of dopants in the ordering of anisotropic media.

KEYWORDS

Cell Wall, Liquid Crystal, Nanoparticle, Dielectric Constant, Refractive Index.

I. INTRODUCTION

It is believed that cells are the smallest building blocks of life. Every cell has a cytoplasm and a cell wall. The cell wall, which is regarded as the cell border, is a coating that envelops the cytoplasm or the contents [1]. The cell wall performs the following functions: bulk transport: exocytosis and endocytosis, markers and signaling, metabolic activities, mechanical structure, defines and encloses the cell, selective permeability, dynamic transport, and so on [2],[3]. As is well known, the cell wall is a dynamic, complex structure made up of a bilayer of phospholipids. The hydrophilic groups cover the inner and outer surfaces of the phospholipids, whereas the hydrophobic ends of the lipids create an intermediate layer. The foundation of membranes is made up of lipid bilayers, and cholesterol may control how fluid the membrane is. Numerous proteins are essential for the operations of the cell membrane, including signal transduction and ion transport [4],[5]. Charged ions and electrons are unable to pass across the wall in large quantities. They may pass across membranes from membrane-spanning protein semiconductors and specialized ion channels, respectively [6]. The anisotropic behavior of

living cell walls has been confirmed by several studies and researches [7]-[9]. Thus, by applying special environmental qualifications, it is achievable to impact the anisotropic properties of the cellular system and induce desired behaviors in it [8]. Properties such as the dielectric properties and physicochemical behavior of cell walls can be improved by taking advantage of this anisotropic property [9]-[11]. There is a large body of published literature demonstrating that the presence of nano-dopants in the environment interacting with the cell walls can affect the above properties [12]-[14]. The extent of these changes depends largely on the shape of the dopants in the environment and their concentration [15].

Substances that flow like liquids but yet have some of the crystals' ordered structure are known as liquid crystals [16],[17]. Molecules in liquid crystals typically exhibit elongation and directionality. Between the crystalline (solid) and isotropic (liquid) phases, there is a unique phase of matter known as the liquid crystal state [18]. Since liquid crystals are anisotropic materials, the system's average alignment with the direction affects its physical characteristics. A high alignment indicates a highly anisotropic material. Likewise, the material is nearly isotropic if the alignment is modest [19].

Nematic liquid crystal materials are characterized by long-range orientation order but lack translational order. A form of optical anisotropy called birefringence is also present in most NLCs (Nematic Liquid Crystals). Birefringence is seen in liquid-crystalline phases because of the parallel order of molecules that exhibit anisotropy in polarizability. The amplitude and sign of the birefringence are determined by the composition and organization of the liquid-crystalline phase and the polarizability properties of the constituent molecules [20],[21]. As previously mentioned, liquid crystals and cell walls share many of the same characteristics, like orientational organization, three-dimensional designs, and anisotropic properties, making them an ideal choice to study the anisotropic behavior of cell walls in the presence of nano dopants [22],[23],[25]. It is also possible to use nanoscale pharmaceutical substances as dopants and study the effect of their presence in different concentrations and morphologies on the anisotropic properties of cell wall [24],[27].

II. EXPERIMENTAL

A. *Materials*

The present study employs 1102 (a mixture of liquid crystal) as an anisotropic environment, similar to the cell wall. LC (Liquid Crystal) 1102 (T_{NI} = 80.5^0 C), is essentially a mixed cyanobiphenyl liquid crystal that is used in both industrial and research applications. The manufacturing company has a patent on the materials that make up Liquid Crystal 1102.

Insoluble nanoparticle, lithium disilicate ($Li_2Si_2O_5$) crystals of 50-60 nm are employed as non-reactive material, while materials containing active agents are used as soluble materials like Retinol ($C_{20}H_{30}O$) (CAS No.68-28-8). Mixtures of the liquid crystal composition and the dopants with different weight ratios (0.1%, 0.3%, and 0.7% w/w%) were prepared. The nano dopants were added to the NLC in the isotropic phase of 1102, and the mixture was sonicated for six hours to complete the doping process and their dielectric constants and refractive indices were measured in a specific temperature range.

B. *Liquid crystal cell preparation*

To create the LC cells, the NP-NLC (Nano Particles- Liquid Crystal) solutions were sandwiched between two 1.2 cm^2 optical glass plates that had transparent electrodes composed of indium tin oxide (ITO) layers. By applying a polyvinyl alcohol surface treatment and rubbing, the sample cells were arranged in a parallel fashion or homogenous orientation. We treated the LC cells' surfaces with lecithin to enable homeotropic alignment. The distance between the electrode surfaces, which was 1µm, was fixed using a Mylar sheet which set the thickness of the liquid crystalline samples. Lastly, epoxy resin glue was employed as a sealing material to attach the plates.

C. *Refractive index measurement*

Abbe's refractometer (*Bellingham Stanley Abbe 60ED*) has been used to measure the refractive index with an accuracy of 0.00001. Abbe's refractor ocular has a polarizer sheet installed to block the unusual rays. This eliminates the boundary line's contrast. Water was circulated in a water bath temperature controller to regulate the temperature of Abbe's refractometer. A thermometer with an accuracy of ±0.01 °C was placed close to the sample to measure the temperature. The extraordinary refractive index, n_e, is too high to be measured with the available refractometer, but the ordinary refractive index, n_o, can be directly measured in the nematic phase. As a result, n_e at every temperature was calculated using $< n >= \frac{1}{3}(n_e + 2n_o)$. The extrapolated average refractive index, or <*n*>, in this case, is the result of extending the isotropic phase's (n_{iso}) refractive index into the range of the nematic phase. Birefringence ($\Delta n = n_e - n_o$) of the nematic phase for the examined LCs was computed using these data.

The order parameter S for the pure liquid crystal sample and the NP-NLC samples (0.1%, 0.3% and 0.7% w/w%) can be computed using the obtained values for the refractive indices and Vuks assumption:

$$S\left(\frac{\Delta\alpha}{\alpha}\right) = \frac{(n_e^2 - n_o^2)}{\langle n^2\rangle - 1} \quad (1)$$

Where $\Delta\alpha = \alpha_e - \alpha_o$ is anisotropy of polarizability and α demonstrates mean molecular polarizability. We exploit $\frac{(n_{e,o}^2 - 1)}{(\langle n^2\rangle + 2)} = \frac{4\pi}{3} N\alpha_{e,o}$ for estimating respective molecular polarizabilities (α_e, α_o) and *N* is the number of molecules per unit volume and $<n^2>$ is defined as $< n^2 >= \frac{1}{3}({n_e}^2 + 2{n_o}^2)$.

Plotting the linear portion of $ln\frac{3({n_e}^2 - {n_o}^2)}{{n_e}^2 + 2{n_o}^2 - 3}$ versus ln $(1 - {}^{T}/_{T_c})$ allows for the determination of $\frac{\Delta\alpha}{\alpha}$, This can be extended to *T=0K*. The scaling factor $\Delta\alpha/\alpha$ is determined by the intercept at *T= 0K*, where a completely ordered structure exists (*S=1*). Order parameter *S* values at various temperatures can be obtained by assuming that $\Delta\alpha/\alpha$ stays constant across all temperatures and entering this value into Eq. (1).

D. *Dielectric measurement*

The dielectric measurements have been performed by an LCR meter having an accuracy of 0.0005. Instek LCR 819, which is combined with a cell temperature controller, the temperature was stabilized with the accuracy of 0.01 °C. For dielectric measurements, a sandwiched capacitance sample with an aligner layer of polymer was utilized. Parallel and perpendicular directions were used to measure the dielectric. At various temperatures, the capacitance values of the sample were ascertained in both its filled and empty forms. Once the impacts of the conductive, ITO layer, and alignment polymer layer are eliminated using Eqs. (2), (3) the change in capacitance will yield the value of the real part of permittivity.

$$\varepsilon_{\parallel} = {}^{C_{\perp}}/_{C_0} \quad (2)$$

$$\varepsilon_{\perp} = {}^{C_{\parallel}}/_{C_0} \quad (3)$$

where $\boldsymbol{C}_{\perp}$ and $\boldsymbol{C}_{\parallel}$ are the oriented LC capacitances perpendicular to and parallel to the cell surface, respectively. $\boldsymbol{C_o}$ is the associated empty cell's capacitance and $\boldsymbol{\varepsilon}_{\parallel}$ and $\boldsymbol{\varepsilon}_{\perp}$ are parallel and perpendicular dielectric constants to the long molecular axis.10 kHz frequencies were used to measure the capacitances.

At various temperatures, the capacitance values of the samples were ascertained in both their filled and empty states. The value of the real part of the constant will be obtained by measuring the change in capacitance after the effects of the conductive, ITO and alignment polymer layers have been eliminated, using Eqs. (2), (3).

III. RESULTS AND DISCUSSIONS

A. *Refractive index studies*

The temperature ranges in which the live cell is stable were used to study the birefringence property and order parameter behavior of pure and doped liquid crystal with soluble and insoluble nano additives at varying concentrations. It is essential to highlight that this study employs a unique nematic liquid crystal for optimal simulation. Unlike typical liquid crystals, this particular substance exhibits an increase in its order parameter as the system's temperature rises within the measured range. This behavior is similar to the response of cell walls in the body's aqueous environment at physiological temperatures. The molecular order changes with temperature, which accounts for the temperature dependency of the birefringence.

The temperature-dependent birefringence of NP-NLC composite systems (0.1%, 0.3%, and 0.7% w/w%) and pure LC systems is displayed in Fig.1. Temperature monitoring of the ordinary and extraordinary refractive indexes (n_o, n_e) of pure and doped liquid crystal 1102 with different concentrations (0.1%, 0.3%, and 0.7% w/w%) of Retinol ($C_{20}H_{30}O$) and $Li_2Si_2O_5$ nanoparticles as soluble and insoluble dopants, in a specific temperature range (310<T<323K) reveals that the extraordinary refractive index in all samples increased significantly with increasing temperature, whereas the coefficient of ordinary refractive index in the same conditions decreased more gently. However, a comparison of data from the pure and doped states of the tested nematic liquid crystal for both of dopants, reveals that the presence of nanoparticles has reduced the

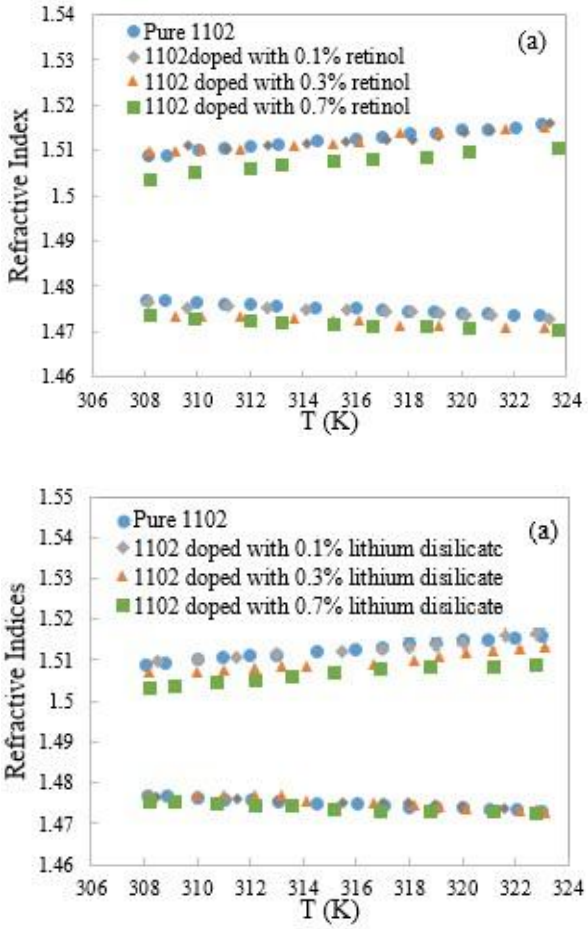

Fig. 1 Temperature monitoring of refractive indices of pure and doped 1102 with (0.1, 0.3, and 0.7% w/w%) retinol (a) and lithium disilicate (b)

ordinary and extraordinary refractive indices and this reduction trend is directly related to an increase in dopant concentration, particularly at higher dopant concentrations.

The birefringence (Δn) values of the pure 1102 LC and composite systems (1102-Retinol), indicate an increasing tendency as the temperature increases in the tested temperature range Fig.2.

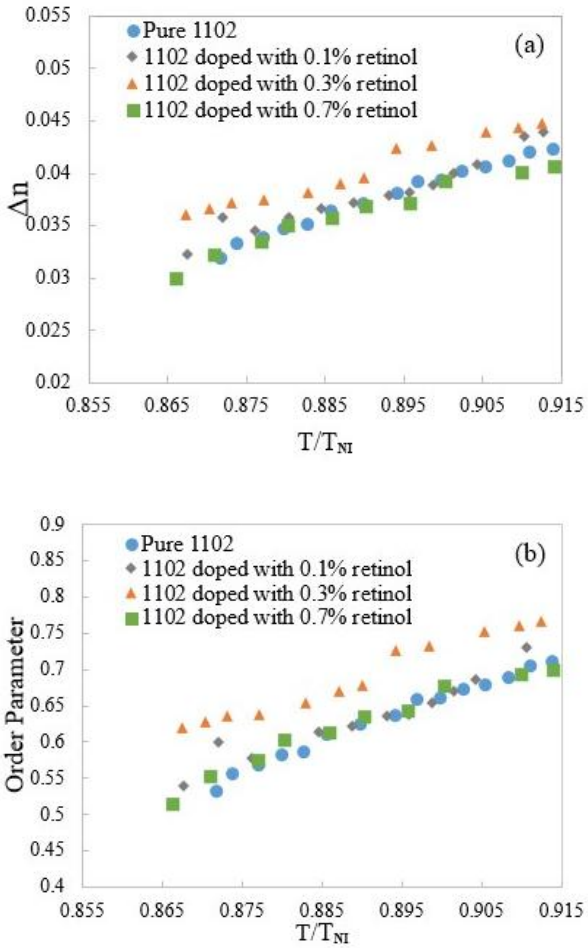

Fig. **2** Temperature monitoring of birefringence (a) and order parameter (b) of pure and doped 1102 with (0.1, 0.3, and 0.7% w/w%) retinol.

Comparing the graphs of changes in the birefringence index and the order parameter of the pure and doped liquid crystal with the mentioned concentrations for Retinol dopants shows that the behavior of these factors in the 1102-retinol mixtures (0.1%, 0.3% and 0.7% w/w%) in the measured temperature range indicate that the presence of Retinol nanoparticles has caused an increase in these values, increases behavior varies depending on the concentration of dopant used. It is evident that, in comparison to the pure state of 1102 LC, the birefringence coefficient and the order parameter of the composition were not significantly affected by the 0.1% Retinol dopant present.

But when the concentration is raised to 0.3%, these parameters noticeably increase. This could be because the compound's intrastructural order is increased as a result of the interaction between the dopant and liquid crystal molecules of 1102, which forms hydrogen bonds between them. As the monitoring continues, a decrease in the order parameter and the birefringence factor can be seen by increasing the dopant concentration to 0.7%. This could be the consequence of an increase in the dopant-dopant intermolecular interactions, which in turn causes a decrease in the order of orientation of the liquid crystal molecules.

In summary, at low concentrations, dopant-dopant interactions are less intense due to fewer particles in the liquid crystal matrix. When the concentration is raised to 0.3%, dopant-dopant interactions increase and hydrogen bonds are formed. At 0.7%, dopant-dopant interactions increase, resulting in aggregation phenomena resembling surfactants. This suggests that retinol's presence in the liquid crystal system resembles surfactant behavior at the Critical Micelle Concentration (CMC) [26].

This alteration demonstrates that the anisotropic liquid crystal structure's internal molecular order is influenced by the presence of dissolved nanoparticles, with the dopant concentration being the primary determinant of this effect.

Put differently, the number of nanoparticles influences the kind of interactions that control the mixture, which alters the molecules' orientation order and results in disruption.

In insoluble doped NLC samples, $Li_2Si_2O_5$ doped NLC samples had a significantly lower order parameter and birefringence index than pure liquid crystal samples Fig. 3.

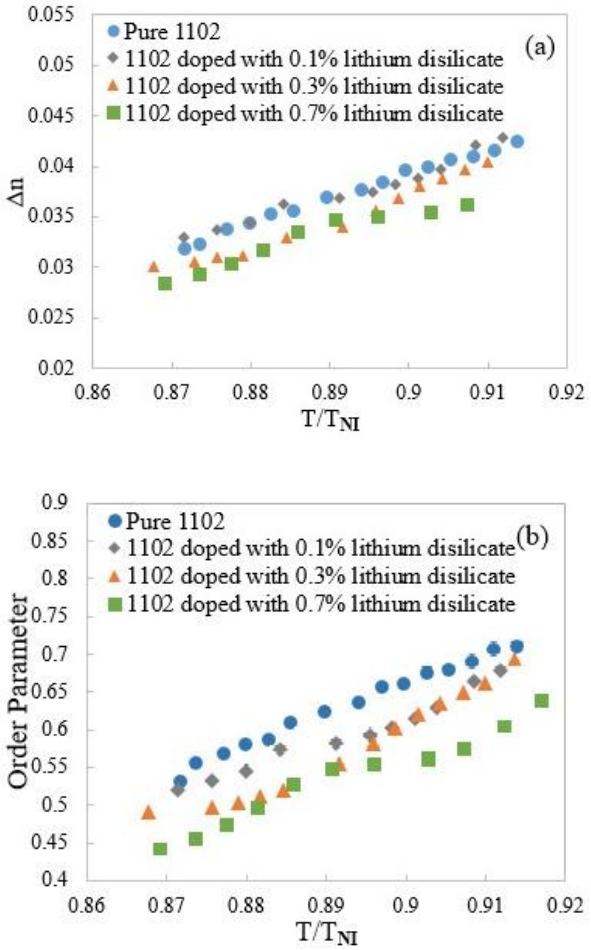

Figure. **3** Temperature monitoring of birefringence (a) and order parameter (b) of pure and doped 1102 with (0.1, 0.3, and 0.7% w/w%) lithium disilicate.

However, the rise in dopant concentration had a relatively low effect on this drop; we did not observe a proportional decrease in the order parameter and birefringence index as the dopant concentration grew to 0.1% w/w%. However, as the concentration and number of dopant particles in the mixtures increase, the effect of steric hindrance of lithium disilicate molecules becomes more apparent, resulting in a decrease in the interaction between the liquid crystal molecules with each other, a disruption in the liquid crystal's internal structural order, and a decrease in the order parameter of NLC doped with 0.3% and 0.7% w/w% lithium silicate compounds.

B. *dielectric properties studies*

Initially, prepared mixtures were placed inside the made cells to test the dielectric constant of the NPs–NLC composites at various concentrations of the Retinol and $Li_2Si_2O_5$ nanoparticles. Next, using Eq. (2) and (3), the dielectric constant of the NPs–LC composites was determined. The dielectric constants' parallel ($\varepsilon_{\parallel}$) and perpendicular ($\varepsilon_{\perp}$) components vary with temperature as seen in Figs. 4 and 5. In the temperature range of the experiment, as the temperature rises, the value of ($\varepsilon_{\parallel}$) falls for the mostly parallel ordering for all samples, as seen in Figs. 4 and 5. But in this temperature range, the ($\varepsilon_{\perp}$) parameter remains nearly constant. ($\varepsilon_{\parallel}$) displays a greater value than ($\varepsilon_{\perp}$) because we employed a positive dielectric anisotropy of the NLC at this point. The dielectric constant of the NPs–NLC composites varies by the presence of NPs at different percentages, as seen by the behavior of the parallel and perpendicular dielectric constant in Figs. 4 and 5.

The data indicates that the incorporation of retinol as a dopant has resulted in an enhancement of both the parallel $\varepsilon_{\parallel}$ and vertical $\varepsilon_{\perp}$ dielectric coefficients in the liquid crystal-retinol mixture. Furthermore, as the concentration of retinol increases, there is a corresponding rise in the positive displacement of these values.

Notably, the liquid crystal 1102 combined with 0.7% w/w% retinol exhibits the most significant increase in the parallel dielectric coefficient. This effect can be attributed to the multiple bonds present in the molecular structure of retinol, which facilitate the electron transfer process when subjected to an electric field. In this case, even while the system order parameter decreases, the aggregation phenomenon at high retinol concentrations leads to the aggregation of polar components, the formation of a bigger dipole, and easier electron transmission in the system.

The investigation into the dielectric properties of 1102 liquid crystal infused with lithium silicate nanoparticles at specified concentrations (0.1%, 0.3%, and 0.7% w/w) reveals that the incorporation of these nanoparticles has led to a decrease in the numerical values of both the parallel and perpendicular ($\varepsilon_{\parallel}$, $\varepsilon_{\perp}$) dielectric coefficients of the liquid crystal composition.

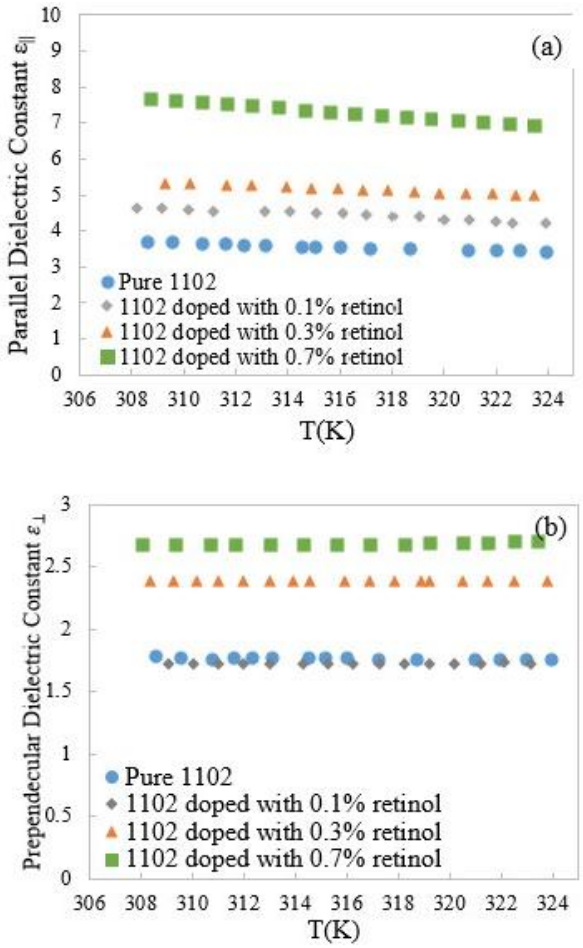

Fig. **4** Temperature monitoring of parallel $\varepsilon_{\parallel}$ (a) and perpendicular $\varepsilon_{\perp}$ (b) dielectric constants of pure and doped 1102 with (0.1, 0.3, and 0.7% w/w%) retinol.

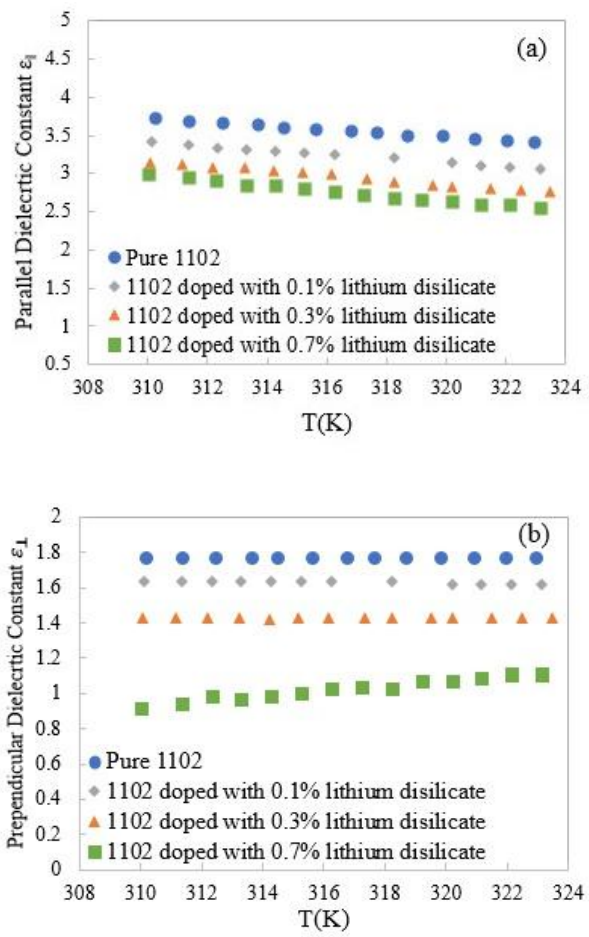

Fig. **5** Temperature monitoring of parallel $\varepsilon_{\parallel}$ (a) and perpendicular $\varepsilon_{\perp}$ (b) dielectric constants of pure and doped 1102 with (0.1, 0.3, and 0.7% w/w%) lithium disilicate.

This reduction is observed to correlate positively with the increasing concentration of the dopant. It is important to note that the orientation of molecules within the liquid crystal matrix and the polarity of molecules are critical factors influencing the dielectric behavior.

Any perturbation in these parameters is likely to result in diminished dielectric coefficients. Consequently, the observed decline in the dielectric coefficients of the lithium disilicate-doped liquid crystal can be attributed to the disruption of intramolecular order and the alteration of intermolecular interactions among the liquid crystal molecules (NLC-NLC), which aligns with theoretical expectations.

It should be noted that, in NP-NLC systems, there are three types of interactions that take place: (I) NLC-to-NLC interaction, (II) NLC-NP interaction, and (III) NPs-NP interaction. Only interactions between NLC molecules occurred in pure NLC [18], [19].

IV. CONCLUSION

This study examined how the shape and concentration of nano dopants influence the photonic and dielectric characteristics of nematic liquid crystals (NLC) which function as simulators for cell walls. Our findings indicate that the incorporation of soluble Retinol into the NLC significantly enhances the order parameter of the NLC-dopants mixture at specific concentrations, leading to an increase in both the parallel ($\varepsilon_{\parallel}$) and perpendicular ($\varepsilon_{\perp}$) dielectric coefficients. The extent of this enhancement is directly related to the concentration of the soluble NPs. Conversely, the introduction of insoluble Lithium Disilicate NPs results in a reduction of the order parameter and dielectric constants of the NLC-NPs mixture, attributed to the geometric configuration of the NPs.

The findings of this study indicate that the dielectric characteristics of the environment used to simulate cell walls can be altered by fine-tuning the concentration and morphology of nanoparticles. Furthermore, given the analogous anisotropic behavior observed in both liquid crystals and cell walls, it can be inferred that the properties of the cell wall may be modulated and predicted by the integration of specific nanoparticles, which differ in their concentration and structural form.

REFERENCES

[1] Kieran J.D. Lee, Susan E. Marcus, and J. Paul Knox, "Cell Wall Biology: Perspectives from Cell Wall Imaging," Molecular Plant, Vol. 4, pp. 212-219, 2011.

[2] Yang NJ and Hinner MJ. "Getting across the cell membrane: an overview for small molecules, peptides, and proteins," Methods Mol Biol. Vol. 1266, pp. 29-53, 2015.

[3] Zachowski A. "Phospholipids in animal eukaryotic membranes: transverse asymmetry and movement," Biochem J. Vol. 294, pp.1–14, 1993.

[4] Kansy M, Senner F, and Gubernator K. "Physicochemical high throughput screening: parallel artificial membrane permeation assay in the description of passive absorption processes," J Med Chem. Vol. 4, pp. 1007–1010, 1998.

[5] Johannes L and Römer W. Shiga toxins "from cell biology to biomedical applications," Nat Rev Microbiol. Vol. 8, pp.105–116, 2010.

[6] Baskin Tobias I. "Anisotropic expansion of the plant cell wall," Annu. Rev. Cell Dev. Biol. Vol, 21, pp. 203-222, 2005.

[7] Landrein, Benoît, and Olivier Hamant. "How mechanical stress controls microtubule behavior and morphogenesis in plants: history, experiments and revisited theories," The Plant Journal, Vol. 75, pp. 324-338, 2013.

[8] M.C. Jarvis and M.C. McCann, "Macromolecular biophysics of the plant cell wall: concepts and methodology," Plant Physiology and Biochemistry, Vol. 38, pp. 1-13, 2000.

[9] Voxeur A. and Herman H. "Cell wall integrity signaling in plants: To grow or not to grow that's the question," Glycobiology, Vol. 26, pp. 950-960, 2016.

[10] Liu, Ke, Zhimao Yang, and Hitoshi Takagi. "Anisotropic thermal conductivity of unidirectional natural abaca fiber composites as a function of lumen and cell wall structure," Composite structures, Vol. 108, pp. 987-991.

[11] Gkolemis K., E. Giannoutsou, ID S. Adamakis, B. Galatis, and P. Apostolakos. "Cell wall anisotropy plays a key role in Zea mays stomatal complex movement: the possible role of the cell wall matrix," Plant Molecular Biology, Vol. 113, pp. 331-351, 2023.

[12] Sendra Marta, P. M. Yeste, Ignacio Moreno-Garrido, José Manuel Gatica, and Julián Blasco, "CeO2 NPs, toxic or protective to phytoplankton? Charge of nanoparticles and cell wall as factors which cause changes in cell complexity," Science of The Total Environment, Vol. 590, pp. 304-315, 2017.

[13] Milewska-Hendel A. Katarzyna S. Weronika G. and Ewa Kurczyńska, "Gold nanoparticles-induced modifications in cell wall composition in barley roots," Cells, Vol. 10, pp. 1965, 2021.

[14] Cui Jianghu, Yadong Li, Qian Jin, and Fangbai Li. "Silica nanoparticles inhibit arsenic uptake into rice suspension cells via improving pectin synthesis and the mechanical force of the cell wall," Environmental Science: Nano Vol. 7, pp. 162-171, 2020.

[15] Das Debabrata, and Giasuddin Ahmed. "Silver nanoparticles damage yeast cell wall," J. Biotechnol, Vol. 3, pp. 36-39, 2012.

[16] Stephen, Michael J. and Joseph P. Straley. "Physics of liquid crystals," Reviews of Modern Physics, Vol. 46, pp. 617, 1974.

[17] R. Kian, M.S. Zakerhamidi, A. Ranjkesh, A.N. Shamkhali, B. Taheri, S.K. Varshney, and T.H. Yoon, "Investigation of the spectroscopic features along with the media polarity effect in some symmetrical disc-shaped liquid crystals," J. Mol. Liq, Vol. 309, pp. 13226, 2020.

[18] A. Ranjkesh, N. Ebrihimpour, M. S. Zakerhamidi, and S. M. Seyedahmadian. "Temperature-dependent dielectric property of a nematic liquid crystal doped with two differently–shaped tungsten oxide (W18O49) nanostructures," Journal of Molecular Liquids Vol. 348, pp. 118024, 2022.

[19] M. S. Zakerhamidi , S. Shoarinejad, and S. Mohammad pour. "Fe_3O_4 nanoparticle effect on dielectric and ordering behavior of nematic liquid crystal host," Journal of Molecular Liquids, Vol. 191, pp. 16-19, 2014.

[20] Sadigh M. Khadem, M. S. Zakerhamidi, and A. Ranjkesh, "Enhanced electro-optical nonlinear responses of doped nematic liquid crystals: Towards optoelectronic devices," Optics and Lasers in Engineering, Vol. 159, pp. 107229, 2022.

[21] Osipov Mikhail A. and Maxim V. Gorkunov, "Nematic liquid crystals doped with nanoparticles: Phase behavior and dielectric properties," In Liquid Crystals with Nano and Microparticles, vol. 2, pp. 135-175. 2017.

[22] Tyagi Yogeshvar, "Liquid crystals: An approach to different state of matter," The Pharma Innovation, Vol. 7, Part H, pp. 540, 2018.

[23] Burrows N. D., Ariane M. Vartanian, Nardine S. Abadeer, Elissa M. Grzincic, Lisa M. Jacob, Wayne Lin, Ji Li, Jordan M. Dennison, Joshua G. Hinman, and Catherine J. Murphy. "Anisotropic nanoparticles and anisotropic surface chemistry," The journal of physical chemistry letters, Vol. 7, pp. 632-641, 2016.

[24] O. Denisova and Y. Abramishvili, "Liquid crystal cell as a model of a biological system: biosensor," E3S Web Conf, International Scientific Conference Ecological and Biological Well-Being of Flora and Fauna. Vol. 420, pp. 09005, 2023.

[25] Yves Bouligand, "Liquid crystals and biological morphogenesis: Ancient and new questions," Comptes Rendus Chimie, Vol. 11, pp. 281-296, 2008.

[26] H. Tajalli, A. Ghanadzadeh Gilani, M.S. Zakerhamidi, M. Moghadam, "Effects of surfactants on the molecular aggregation of rhodamine dyes in aqueous solutions," Spectrochimica Acta Part A: Molecular and Biomolecular Spectroscopy, Vol. 72, pp. 697-702, 2009.

[27] Nechipurenko Yu , Ryabokon, VF , Semenov Sergei , and Evdokimov YM. "Thermodynamic models describing the formation of "bridges" between, molecules of nucleic acids in liquid crystals, " Biofizika. Vol. 48. pp. 635-643, 2003.

THIS PAGE IS INTENTIONALLY LEFT BLANK.